CAD Tool for Burn Diagnosis

Begoña Acha[1], Carmen Serrano[1], José I. Acha[1], Laura M. Roa[2]

[1]Área de Teoría de la Señal y Comunicaciones, Escuela Superior de Ingenieros, University of Seville, Camino de los Descubrimientos s/n, 41092 Seville, Spain.
{bacha, cserrano, acha}@us.es
[2]Grupo de Ingeniería Biomédica, Escuela Superior de Ingenieros, University of Seville, Camino de los Descubrimientos s/n, 41092 Seville, Spain.
laura@us.es

Abstract. In this paper a new system for burn diagnosis is proposed. The aim of the system is to separate burn wounds from healthy skin, and the different types of burns (burn depths) from each other, identifying each one. The system is based on the colour and texture information, as these are the characteristics observed by physicians in order to give a diagnosis. We use a perceptually uniform colour space ($L^*u^*v^*$), since Euclidean distances calculated in this space correspond to perceptually colour differences. After the burn is segmented, some colour and texture descriptors are calculated and they are the inputs to a Fuzzy-ARTMAP neural network. The neural network classifies them into three types of burns: superficial dermal, deep dermal and full thickness. Clinical effectiveness of the method was demonstrated on 62 clinical burn wound images obtained from digital colour photographs, yielding an average classification success rate of 82 % compared to expert classified images.

1 Introduction

For a successful evolution of a burn injury it is essential to initiate the correct first treatment [1]. To choose an adequate one, it is necessary to know the depth of the burn, and a correct visual assessment of burn depth highly relies on specialized dermatological expertise. As the cost of maintaining a Burn Unit is very high, it would be desirable to have an automatic system to give a first assessment in all the local medical centres, where there is a lack of specialists [2], [3]. The World Health Organization demands that, at least, there must be one bed in a Burn Unit for each 500000 inhabitants. So, normally, one Burn Unit covers a large geographic extension. If a burn patient appears in a medical centre without Burn Unit, a telephone communication is established between the local medical centre and the closest hospital with Burn Unit, where the not-expert doctor describes subjectively the colour, shape and other aspects considered important for burn characterization. The result in many cases is the application of an incorrect first treatment (very important, on the other hand, for a correct evolution of the wound), or unnecessary displacements of the patient, involving high sanitary cost and psychological trauma for the patient and family.

With the fast advances in technology, the Computer Aided Diagnosis (CAD) systems are getting more popular. However, nowadays, the research in the field of colour skin images is being developed slowly due to the difficulty of translating colour human perception into objective rules, analyzable by a computer. That is why automation of burn wound diagnosis is still an almost unexplored field. While there is hardly bibliography about burn depth determination by visual image analysis and processing [4] [5], one can find some research about the relationship between depth and superficial temperature [6], or other works trying to evaluate burn depth by using thermographic images [7], infrared and ultraviolet images [8], radioactive isotopes [9] and Doppler laser flux measurements [10]. These techniques have limitation not only in diagnosis accuracy but also in unallowable economical cost.

Talking more generally about colour skin image processing, one can find two main applications in the literature [11]: the assessment of the healing of skin wounds or ulcers [12-16], and the diagnosis of pigmented skin lesions such as melanomas [17-20]. The analysis of lesions involves more traditional image processing techniques such as edge detection and object identification, followed by an analysis of the size, shape, irregularity and colour of the segmented lesion. However, in wound analysis, although it is necessary to detect the wound border and to calculate its area, analysis of the colours within the wound site is often more important. Particularly, in the case of burn depth determination, we are not going to focus on the shape of the burn, because it is irrelevant in order to predict its depth. The main characteristics for this purpose are the colour and texture information, as they are what physicians observed in order to give a diagnosis.

The developed system consists of the following steps:

1. Image acquisition. We have developed a new protocol for standardizing the image acquisition [2] [3].
2. Segmentation. Many segmentation algorithms have been proposed in the literature, but none of them can be used as a standard, because most of them are highly application dependent [21]. Particularly, when segmenting burn wounds, general-purpose segmentation algorithms are less effective because there are only slight differences between healthy and burnt skin, whereas there are other significant borders in the image. That is the reason why in this paper we proposed a new segmentation algorithm, which has been proven effective in segmenting burn wound images. Section 2 is devoted to describe this new algorithm.
3. Classification. Once the burnt part is segmented, we extract from it representative colour and texture descriptors, which will be the entries to a neural network classifier that will give the depth. We explain feature extraction and classification in Section 3.

2 Image Acquisition

The image acquisition is carrying out by means of a digital photographic camera. The reasons for this choice are mainly due to its low cost to make feasible its practical implementation and its easy use. Any non-specialised person must be able to acquire data from the patient, because it is not possible to have an expert in each centre.

Once the acquisition system is selected, we had to specify a protocol to acquire the image, that is, we have to develop a protocol to homogenise the patient information that should go with each photograph and another one about the way of taking the photograph. Medical specialists made the first one [2]. To determine the second one a pilot study was done, where an interdisciplinary group composed by burn specialists and non-specialists filled out questionnaires about image quality [2] [3]. The main points in the resulting protocol were: distance between camera and patient approximately of 40 cm, it should appear healthy skin in the image, the background should be a green/blue sheet (the ones used in hospitals), the flash has to be on, the camera should be placed parallel to the burn.

As with this system what we want to solve is the problem of diagnosing when a patient arrives to the local medical centre in order to receive an adequate first treatment, all the images used for validating our algorithms have been taken by physicians within 24 hours of burn evolution.

It should be noted that we have tried to do the procedure as easier as possible for physicians, what may mean that we have got more difficult images in order to automatically analyse them. First of all and trying to be closer to a hypothetic practical implementation of the system, the physicians, instead of us, took the photographs. Depending on the room where the physicians took the photographs, the illumination was different (some rooms had windows and some not). All of them have typical fluorescent lights and to try to homogenise as much as possible the illumination the flash had to be always on, so that the main quantity of light came from it. The camera was a digital Canon Power Shot 600.

3 Segmentation Algorithm

The new colour segmentation algorithm that is proposed consists of four main steps:

1. Preprocessing step.
2. Conversion to a single channel image, where a pixel value is a measure of the similarity of its colour to the one to be segmented.
3. Automatic thresholding to achieve the segmented image.
4. Postprocessing step.

It must be emphasized that the colour to be segmented is obtained from a selection box that the user has to select with the mouse. As it was pointed out in [22], it is very difficult to develop a completely automatic system. The reason lies on the normal and healthy skin colour properties. There is a large variability in the healthy skin, even within the same human race. On the other hand, for a non-expert physician, in fact for many people, it is easy to differentiate burnt skin from normal one, due to the experience. The problem is to differentiate among the different depths of the burn. We have represented some colour descriptors (H, S, u^*, v^*,...) of fifty 49×49 pixel images, belonging to both normal and burnt skin. In Figure 1a the chromatic coordinates of the $L^*u^*v^*$ colour space are represented, and in Figure 1b the saturation versus the hue coordinates are shown. It can be seen that there is a large variability in the colour coordinates for the 50 small images of healthy skin, as well as a strong overlap among

healthy skin, blisters (superficial dermal) and brown-coloured full thickness burns[1]. Therefore, we can conclude that it is necessary the help of the user by selecting the colour of the burn to be segmented.

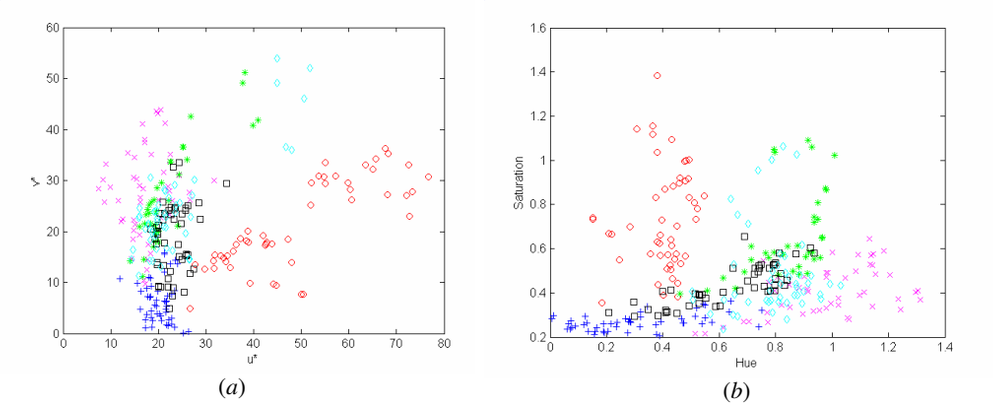

(*a*) (*b*)

Fig. 1. (*a*) Comparison of u^* and v^* colour coordinates for 50 burn images per depth and healthy skin, where (o) is superficial dermal (red), ( ) is superficial dermal (blisters), (+) is deep dermal, (x) is full thickness (creamy), (*) is full thickness (brown) and (◊) is healthy skin. (*b*) The same for saturation and hue coordinates

3.1 Preprocessing Step

Before segmenting the image, it is preprocessed to make the regions more homogeneous. Therefore a low pass filter is required. But this filter must exhibit the property of preserving edges unaltered. A filter that fit these two requirements is the anisotropic diffusion filter [23]. Other low-pass filters, like gaussian, tend to blur the whole image, losing border locations.

In order to perform the anisotropic diffusion, we follow the idea developed by Lucchese and Mitra of separating the diffusion of the chromatic and achromatic information [24] [22]. It calculates the hue and chroma components from the $L^*u^*v^*$ colour coordinate system. Once it has these two chromatic components, it forms a complex quantity as $P = c \cdot \exp(jh)$, where c and h denotes the chroma and hue components respectively. The anisotropic diffusion is carried out by means of the partial differential equations explained in [24] for the P and the lightness (L^*) components. We have proven experimentally that doing the diffusion separately for the chromatic and achromatic channels yields better results than diffusing in the R, G and B planes.

[1] There are three main depths of burns that can present five different appearances: superficial dermal (bright red colour or presence of blisters (usually brown colour)), deep dermal (pink-whitish colour) and full thickness (beige-yellow colour or dark brown colour).

3.2 Single Channel Image Conversion

In this step a grey scale image is obtained from the diffused colour image. To this aim, the $L^*u^*v^*$ diffused image must be transformed to a measure which, for each pixel, is proportional to the similarity to the colour to be segmented.

The single channel image is based on the Euclidean distance from a colour pixel to the centroid of the selection box selected by the user. To take into account the texture information, instead of calculating the distance from a pixel to a particular colour, we calculate the distance from a group of pixels to a mask of size L×L. The mask represents a selection box in the area to be segmented, that is, a small selection done with the mouse by the user in the burnt part of the image. This selection box must be slid as a mask along the image and, for the pixel in the centre of the mask position, the following operation must be performed:

$$f(n,m) = \sum_{i=n-\Delta}^{n+\Delta} \sum_{j=m-\Delta}^{m+\Delta} d(p(i,j), w(i,j)) , \quad (1)$$

where $\Delta = (L-1)/2$ (L odd), $p(i,j)$ represents a pixel in the image to be segmented in $L^*u^*v^*$ colour coordinates, $w(i,j)$ is a pixel of the mask of size L×L, and $d(\cdot)$ represents the Euclidean distance between pixels $p(i,j)$ and $w(i,j)$.

3.3 Thresholding Operation

After applying the former algorithm, we have a grey scale image where pixels with lowest values are those in the region to be segmented. As this image has been carefully designed to emphasize the burnt regions, a thresholding operation should suffice to get a good segmentation. Therefore, a thresholding process is applied to this grey scale image in order to get the segmented area.

There are two possibilities to carry out the thresholding:

1. The user introduces the threshold manually. Most of the segmentation algorithms in the literature work this way. Depending on the application, and normally on the image, the threshold varies.
2. Automatic threshold selection. This is the most desired way to solve the thresholding problem, although the most difficult. But, as we are involved in a particular application and with images following a specific protocol, the finding of an automatic threshold is easier to carry out. Actually, there are some general purpose algorithms that do not need the introduction of a threshold. They usually give good results when the colours of the image are well differentiated. In our case, the colours of the different burn depths and healthy skin are very close to each other, so the application of this kind of algorithms does not yield good results.

In previous works we have tested the images with manual thresholding. The results were very good, which is normal, because we can choose the best threshold for each image [25]. In further studies we developed an automatic thresholding algorithm consisting in applying a modification of Otsu's method [22]. Results in these cases were also very good, but this algorithm is specific for the type of images we are working with, because it makes the assumption that the histogram has three main peaks: the most right one belonging to the background, the one in the middle belonging to the healthy skin, and the most left one belonging to the burnt skin. So, in case that the image does not follow the protocol correctly or that there is more than one type of burn in the same photograph, the algorithm may fail.

In this work we present a new thresholding algorithm that can be useful not only for this kind of images, but for any type of image. It uses Otsu's method, but with a previous step to find peaks in the histogram.

As the input image for thresholding is a grey scale image where pixels with the lowest values belong to the region to be segmented, we want to determine the threshold which isolates the most left significant peak in the histogram. In order to carry out this task we first automatically find the most significant peaks in the histogram. The algorithm that finds these peaks is summarized in the following steps:

1. Find all peaks in the histogram.
1. Select the peaks in the new curve formed by the peaks found in step 1.
2. Remove non-significant peaks. Those peaks whose values are less than 1% of the maximum peak value are rejected.
3. Remove non-significant valleys. We calculate the minimum value of the pixels between two peaks. If this minimum is greater than 75% of the minimum peak value out of the two peaks, then no significant valley is considered.

Once we have found all the significant peaks in the histogram, we know that the threshold found will be between the two most left peaks in the histogram. To find this threshold, Otsu's method is applied to the histogram between these two peaks. Otsu's method is an adaptive thresholding technique to split a histogram into two classes [26].

3.4 Postprocessing Step

With this processing step, the segmentation result is smoothed by removing small points that differ from their surroundings. To this end, a median filtering has been employed.

4 Classification Part

Once the burn is segmented, we have to classify it into its depth. It has been proven that physicians determine the depth of a burn based on color perception, as well as on some texture aspects. This implies that if a color metric in accordance with human perception is applied, we will get a color feature adequate to attain our goal of classifying bum wounds. One of the color representation based on human color

matching is the CIE $L^*u^*v^*$ color space, since it was designed so that intercolor distances computed using the $\|\cdot\|_2$ norm correspond to subjective color matching data.

In this study, we have employed a set of descriptors formed by first order texture parameters extracted from the three coordinates of the $L^*u^*v^*$ color space as well as from the hue and chroma measurements derived from them. More specifically, the descriptors chosen are: mean of lightness (L^*), mean of hue (h), mean of chroma (c), standard deviation of lightness (σ_L), standard deviation of hue (σ_h), standard deviation of chroma (σ_c), mean of u^*, mean of v^*, standard deviation of u^* (σ_u), standard deviation of v^* (σ_v), skewness of lightness (s_L), kurtosis of lightness (k_L), skewness of u^* (s_u), kurtosis of u^* (k_u), skewness of v^* (s_v) and kurtosis of v^*.

Afterwards it has been necessary to apply a descriptor selection method to obtain the optimum set for the subsequent classification.

4.1 Feature Selection

The discrimination power of these 16 features is analyzed using the *Sequential Forward Selection* (SFS) method and the *Sequential Backward Selection* (SBS) method [27] via the Fuzzy-ARTMAP neural network which is detailed in the following subsection.

SFS is a bottom-up search procedure where one feature at a time is added to the current feature set. At each stage, the feature to be included in the feature set is selected among the remaining available features which have not been added to the feature set. So the new enlarged feature set yields a minimum classification error comparing to adding any single feature. The algorithm stops when adding a new feature yields an increase of the classification error.

The SBS is the top-down counterpart of the SFS method. It starts from the complete set of features and, at each stage, the feature which shows the least discriminatory power is discarded. The algorithm stops when removing another feature implies an increase of the classification error.

To apply these two methods we have fifty 49×49 pixel images per each appearance (as there are five appearances, in all we have 250 49×49 pixel images)[2]. The selection performance is evaluated by fivefold cross validation (XVAL) [28]. In this sense, the disadvantage of sensitiveness to the order of presentation of the training set, that the SBS and SFS methods present [27], is diminished. To perform the XVAL method the 50 images per burn appearance are split into five disjoint subsets. Four of these subsets (that is, 40 images per appearance) serve as training set for the neural network, while the other one (10 images) is used as validation set. Then, the procedure is repeated interchanging the validation subset with one of the training subsets, and so on till the five subsets have been used as validation sets. The final classification error is calculated as the mean of the errors for each XVAL run.

The results of applying the SFS and SBS methods are summarized in Table 1. The average error is calculated counting the misclassifications and dividing by the total

[2] The 250 49×49 pixel images are small images showing each one only one burn appearance (no healthy skin or background). Each 49×49 pixel image has been validated by two physicians as belonging to a particular depth.

number of images used to validate. Looking at Table 1 we choose the SBS feature set (lightness, hue, standard deviation of the hue component, u^* chrominance component, standard deviation of the v^* component, skewness of lightness) as the entries to the neural network, due to the smaller average error.

Table 1. Results of SFS and SBS methods for feature selection

Method	Feature set	Average error
SFS	$L^*, H, \sigma_C, u^*, v^*, \sigma_v, s_L$	2%
SBS	$L^*, H, \sigma_H, u^*, \sigma_v, s_L$	1.6%

4.2 Fuzzy-ARTMAP Neural Network

The classifier used is a Fuzzy-ARTMAP neural network. This type of network is based on the Adaptive Resonance Theory developed by Grossberg and Carpenter. Fuzzy-ARTMAP is a supervised learning classification architecture for analog-value input pairs of patterns [29]. The reasons for this choice are that Fuzzy-ARTMAP offers the advantages of well-understood theoretical properties, an efficient implementation, clustering properties that are consistent with human perception, and a very fast convergence. It has also a track record of successful use in industrial and medical applications [30]. Other strongpoints of this type of neural network are the small number of design parameters (the vigilance parameter, $\rho_a \in [0,1]$, and the selection parameter, $\alpha>0$) and that the architecture and initial values are always the same, independent of the application.

The input parameters are the features selected by the SBS method (L^*, H, σ_H, u^*, σ_v, s_L). The network classifies them into five regions (the first and the second belonging to superficial dermal depth, the third to deep dermal, and the fourth and fifth to full-thickness). So, the network has six neurons in the input layer, five neurons in the hidden layer and five neurons in the output layer.

5 Experimental Results

This burn CAD tool was tested with 62 images (Caucasian race). The images are digital photographs taken by physicians following the acquisition protocol. All the images were diagnosed by a group of plastic surgeons, affiliated to the Burn Unit of the Virgen del Rocío Hospital, from Seville (Spain). The assessments were validated one week later, as it is the common practice when handling with burned patients.

5.1 Segmentation Results

Figs. 2 to 4 show the segmentation results for some images of the three types of depth. Figs. *a* represent original images and Figs. *b* represent the segmented ones. In

the segmented images we have marked with yellow colour the segmented region. In all the cases, the burn wound was segmented correctly from the normal skin. We have fixed the number of times the image is diffused to 10.

5.2 Classification Results

Classification results are summarized in Table 2. We have used 22 images with superficial dermal burns, 18 with deep dermal burns and 22 with full-thickness burns. The average success percentage was 82.26%.

Table 2. Classification results

Burn depth	**Success percentage**
Superficial dermal	86.36%
Deep dermal	83.33%
Full-thickness	77.27%
Average	**82.26%**

All superficial dermal burns misclassified were classified by the network as deep dermal ones. All deep dermal burns were misclassified as superficial dermal ones. In general, this is also common among physicians; actually some burns are diagnosed as "intermediate depth", when they are neither clearly superficial dermal nor deep dermal. For these burns it is necessary to wait one week in order to get the definitive assessment.

(*a*) (*b*)

Fig. 2. Segmentation result for a superficial dermal burn. (*a*) Original image where the selection box selected by the user is shown in red. (*b*) Segmented image

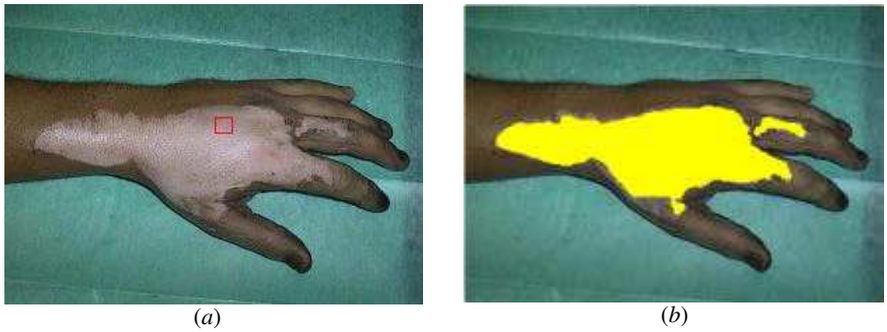

(*a*) (*b*)

Fig. 3. Segmentation result for a deep dermal burn. (*a*) Original image where the selection box selected by the user is shown in red. (*b*) Segmented image

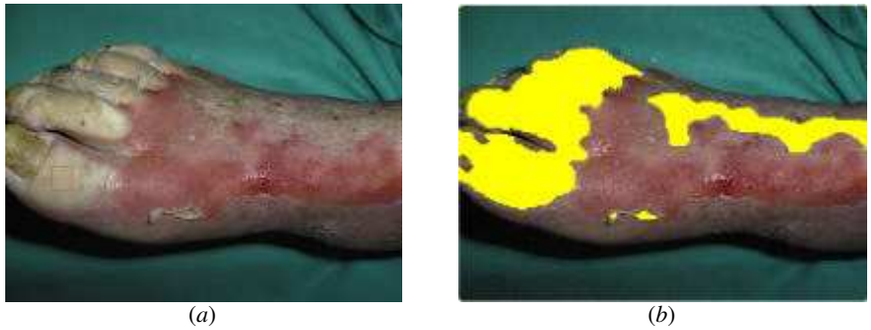

(*a*) (*b*)

Fig. 4. Segmentation result for a full thickness burn. (*a*) Original image, which have both superficial dermal burn (the red part) and full-thickness burn (the whitish part). (*b*) Segmented image. In this case the user has selected a small box in one toe in order that the algorithm segments all the full thickness part of the burn. It segments correctly all the full thickness parts of the image regarding what physicians said.

6 Discussion and Conclusions

In this paper a color image segmentation and classification method is proposed in order to determine the depth of a burn. We use digital color photographs taken by the physicians following a determined protocol.

The system starts with a segmentation step, whose aim is to isolate the burn wound from the rest of the scene (healthy skin and background). In order to perform this step, we start with a preprocessing step (diffusion filtering and change of color space). Then a transformation from a three-plane image ($L^* u^* v^*$) to one-plane image is performed, where it is taken into account color and texture information. From the

gray-scale image a threshold is determined automatically to separate the burn from the background. The last processing step consists in a median filtering to homogenize regions. The segmentation algorithm works well for most of the database images, and it is useful not only for the images shown here that follow a specific protocol, but also for any kind of images.

Once the burn is isolated, we extract from it six color and texture descriptors that will be the inputs to the classifier. The selection of the features has been carried out by the Sequential Forward and Backward Selection methods. We start from 16 texture and color characteristics and after applying the Sequential methods we get the six descriptors with the largest discrimination power.

The six descriptors are the inputs to a Fuzzy-ARTMAP neural network which classified them as one of the possible depths a burn can present. We tested 62 photographs, yielding a classification average success percentage of 82.26%. Based on these results, we can conclude that our method shows a very good performance for segmenting and classifying the images into their burn depths.

Acknowledgments

The authors thank Dr. Gómez-Cía, Dr. Torre and the Burn Unit of Virgen del Rocío Hospital, Seville (Spain), their invaluable help, for providing us the burn wound photographs and their medical advice.

References

1. Clarke, J.A.: A Colour Atlas of Burn Injuries. Chapman & Hall Medical, London (1992)
2. Serrano, C., Roa, L.M., Acha, B.: Evaluation of a Telemedicine Platform in a Burn Unit. Proc. IEEE Int. Conf. on Information Technology Applications in Biomedicine, Washington (1998) 121-126
3. Roa, L.M., Gómez-Cía, T., Acha, B., Serrano, C.: Digital Imaging in Remote Diagnosis of Burns. Burns, **7** (1999) 617-624
4. Afromowitz, M.A., Van Liew, G.S., Heimbach, D.M.: Clinical Evaluation of Burn Injuries Using an Optical Reflectance Technique. IEEE Trans. on Biomedical Engineering, **2** (1987) 114-127
5. Afromowitz, M.A., Callis, J.B., Heimbach, D.M., DeSoto, L.A., Norton, M.K.: Multispectral Imaging of Burn Wounds: A New Clinical Instrument for Evaluating Burn Depth. IEEE Trans. on Biomedical Engineering, **10** (1988) 842-850
6. Wyllie, F.J., Sutherland, A.B.: Measurement of Surface Temperature as an Aid to the Diagnosis of Burn Depth. Burns, **2** (1991) 123-127
7. Cole, R.P., Jones, S.G., Shakespeare, P.G.: Thermographic Assessment of Hand Burns. Burns, **1** (1990) 60-63
8. Barsley, R.E., West, M.H., Fair, J.A.: Forensic Photography. Ultraviolet Imaging of Wounds on Skin. American Journal of Forensic Medical Pathology, **4** (1990) 300-308
9. Bennett, J.E., Kingman, R.O.: Evaluation of Burn Depth by the Use of Radioactive Isotopes – An Experimental Study. Plastic and Reconstructive Surgery, **4** (1957) 261-272
10. Niazi, Z.B.M., Essex, T.J.H., Papini, R., Scott, D., McLean, N.R., Black, J.M.: New Laser Doppler Scanner, a Valuable Adjunct in Burn Depth Assessment. Burns, **6** (1993) 485-489

11. Berriss, W.P., Sangwine, S.J.: Automatic Quantitative Analysis of Healing Skin Wounds using Colour Digital Image Processing. http://www.smtl.co.uk/World-Wide-Wounds/1997/july/Berris/Berris.html#perednia1. (1997)
12. Herbin, M., Bon, F.X., Venot, A., Jeanlouis, F., Dubertret, M.L., Dubertret, L., Strauch, G.: Assessment of Healing Kinetics through True Color Image Processing. IEEE Trans. on Medical Imaging, **1** (1993)
13. Arnqvist, J., Hellgren, L., Vincent, J.: Semiautomatic Classification of Secondary Healing Ulcers in Multispectral Images. Proc. of 9th International Conference on Pattern Recognition, Rome (1988) 459-461
14. Hansen, G.L., Sparrow, E.M., Kokate, J.Y., Leland, K.J., Iaizzo, P.A.: Wound Status Evaluation using Color Image Processing. IEEE Trans. on Medical Imaging, **1** (1997) 78-86
15. Liu, J., Bowyer, K., Goldgof, D., Sarkar, S.: A Comparative Study of Textures Measures for Human Skin Treatment. Proc. of Int. Conf. on Information, Communications and Signal Processing ICICS'97, Singapur (1997) 170-174
16. Mekkes, J.R., Westerhof, W.: Image Processing in the Study of Wound Healing. Clinics in Dermatology, **4** (1995) 401-407. Summarized in: http://www.ncbi.nlm.nih.gov/htbin-post/Entrez/query?uid=8665449&form=6&db=m&Dopt=r
17. Fiorini, R.A., Crivellini, M., Codagnone, G., Dacquino, G.F., Libertini, G., Morresi, A.: DELM Image Processing for Skin-Melanoma early Diagnosis. Proc. SPIE – Int. Soc. Opt. Eng. Vol. 3164 (1997) 359-370
18. Thira, J.P., Macq, B.: Morphological Feature Extraction for the Classification of Digital Images of Cancerous Tissues. IEEE Trans. on Biomedical Engineering, **10** (1996) 1011-1020
19. Hance, G.A., Umbaugh, S.E., Moss, R.H., Stoecker, W.V.: Unsupervised Color Image Segmentation with Application to Skin Tumor Borders. IEEE Engineering in Medicine and Biology. Jan/Feb (1996) 104-111
20. Zhang, Z., Stoecker, W.V., Moss, R.H.: Border Detection on Digitized Skin Tumor Images. IEEE Trans. on Medical Imaging, **11** (2000) 1128-1143
21. Pratt, W.K.: Digital Image Processing. 3rd edn. Wiley, New York (2001)
22. Serrano, C., Acha, B., Acha, J.I.: Segmentation of Burn Images based on Color and Texture Information. Proc. SPIE Int. Symposium on Medical Imaging, San Diego (CA, USA). (2003). To be published
23. Perona, P., Malik, J.: Scale-Space and Edge Detection using Anisotropic Diffusion. IEEE Trans. on Pattern Analysis and Machine Intelligence, **7** (1990) 629-639
24. Lucchese, L., Mitra, S.K.: Color Segmentation based on Separate Anisotropic Diffusion of Chromatic and Achromatic Channels. IEE Proc. Vision, Image and Signal Processing, **3** (2001) 141-150
25. Acha, B., Serrano, C., Acha, J.I.: Segmentation of Burn Images Using the $L^*u^*v^*$ Space and Classification of their Depths by Color and Texture Information. SPIE Int. Symposium on Medical Imaging, San Diego (CA, USA.). Vol. 4684, Part Three (2002) 1508-1515
26. Petrou, M., Bosdogianni, P.: Image Processing. The Fundamentals. Wiley, Chichester (U.K.) (1999)
27. Fukunaga, K.: Introduction to Statistical Pattern Recognition. 2nd edition, Morgan Kaufmann (Academic Press), San Diego, CA, (1990)
28. Ganster, H., Pinz, A., Röhrer, R., Wilding, E., Binder, M., Kittler, H.: Automated Melanoma Recognition. IEEE Trans. on Medical Imaging, **3**, (2001) 233-239
29. Carpenter, G.A., Grossberg, S., Markuzon, S., Reynolds, J.H.: Fuzzy-ARTMAP: A Neural Network Architecture for Incremental Supervised Learning of Analog Multidimensional Maps. IEEE Trans. on Neural Networks, **5** (1992) 698-713
30. Donohoe, G.W., Nemeth, S., Soliz, P.: ART-based Image Analysis for Pigmented Lesions of the Skin. 11th IEEE Symposium on Computer-Based Medical Systems, (1998) 293-298